ISSN 1028-334X, Doklady Earth Sciences, 2007, Vol. 417A, No. 9, pp. 1412–1415. © Pleiades Publishing, Ltd., 2007.
Original Russian Text © A.A. Marakushev, N.G. Zinovieva, L.B. Granovsky, 2007, published in Doklady Akademii Nauk, 2007, Vol. 417, No. 5, pp. 673–676.

GEOCHEMISTRY

Genetic Types of Ultrahigh-Pressure Minerals in Meteorites

Academician of the RAS **A. A. Marakushev,**
N. G. Zinovieva, and L. B. Granovsky

Received June 4, 2007

DOI: 10.1134/S1028334X07090255

Minerals formed in natural processes at a very high pressure serve as indicators for the genetic interpretation of both terrestrial rocks and meteorites. They contain, at least, three types of ultrahigh-pressure (UHP) minerals with principally different modes of occurrence and paragenetic relations: (1) minute diamond grains (up to 10 nm in size) that are overfilled with fluid hydrogen inclusions in association with moissanite (SiC) and incorporated into a kamacite matrix of chondrites of all chemical groups; (2) larger (10–10 000 nm) diamond grains enriched in fluid inclusions in association with daubreelite, troilite, and moissanite within kamacite injections into ureilites; and (3) ringwoodite, wadsleyite, majorite, and others in glassy veinlets within brecciated chondrites. The main stages of the evolution of the iron–stony meteoritic material of the solar system are recorded in the UHP minerals listed above.

(1) Diamonds in the kamacite matrix of chondrites are characterized by an abundance of fluid inclusions such that the bulk density of diamond grains equals 2.2 g/cm^3, whereas the density of pure diamond is 3.5 g/cm^3. The fluids are distinguished by a high ^{136}Xe/^{134}Xe ratio equal to 1.04 in diamonds from carbonaceous chondrites. This value is similar to the ratio in Jupiter's atmosphere measured by the Galileo probe in 1996 [7]. In the solar wind, this ratio is only 0.80. The xenon ratio mentioned above confirms our suggestion [1] that chondritic melts were formed as dense cores of the parental giant planets similar to Jupiter under a very high pressure created by their fluid shells. This pressure controlled not only the formation of fluid diamond nuclei, but also the anomalous distribution of oxygen isotopes between chondrules and the diamond-bearing matrix ($\tan\alpha = 1$) inherent to the so-called protoplanet evolution of chondritic magmatism in the interiors of giant protoplanets. The evolution resembled the normal mass fractionation of oxygen isotopes ($\tan\alpha = 0.5$) during the subsequent crystallization of chondrites at the planet stage after pressure release due to the loss of giant shells by protoplanets and the transformation of their cores into autonomous planets. The loss of giant fluid shells by protoplanets was related to the impact of the young Sun that had a higher energetic level in comparison with its present-day state. The enormous pressure differential in the evolution of chondrites is recorded in all their chemical groups as a combination of isotopically anomalous UHP minerals (diamond and moissanite) with volcanic glass and low-pressure minerals that are characterized by normal mass fractionation of oxygen isotopes. This combination defines chondrites as polyfacies rocks formed within a wide pressure range [2]. However, the pressure regime in the evolution of iron–stony planets is complicated by the presence of their kamacite cores, which were formed still at the protoplanet stage under a very high fluid pressure and therefore concentrated enormous reserves of high-density fluids. At the planet stage, these cores became sources of internal pressure responsible for the stressed state that gave rise to the explosive breakdown of planets into asteroids and meteorites. However, prior to this breakdown, the stressed state of the planets, which were consolidating from the surface, was realized in their endogenic activity related to the impact of fluid cores on the silicate shells of planets. In meteorites, this process is recorded in primitive pigeonite–olivine achondrites (ureilites) that contain complex injections of fluid- and diamond-bearing kamacite melts.

(2) In ureilites, diamonds form larger grains (up to 10 000 nm in size), which are enriched in fluid inclusions. In Fig. 1, genetically different diamonds are compared with respect to the content of noble gas isotopes. The terrestrial diamonds are distinguished from diamonds hosted in meteorites, which have incomparably higher contents of noble gases as a response to their formation under a much higher pressure. Diamonds

---

Department of Petrology, Faculty of Geology, Moscow State University, Leninskie gory, Moscow, 119991 Russia; e-mail: zinov@geol.msu.ru

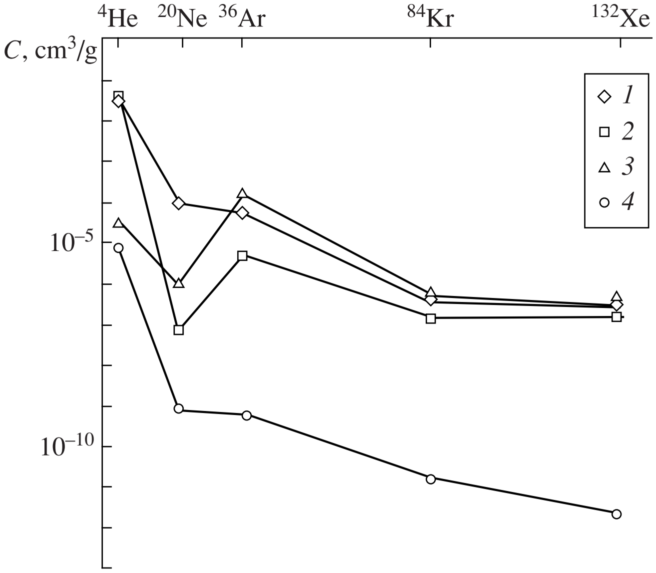

Fig. 1. Noble gas contents in (*1*) diamond and (*2*) moissanite from a carbonaceous chondrite matrix [5, 6], (*3*) ureilite [4], and (*4*) terrestrial diamond [9].

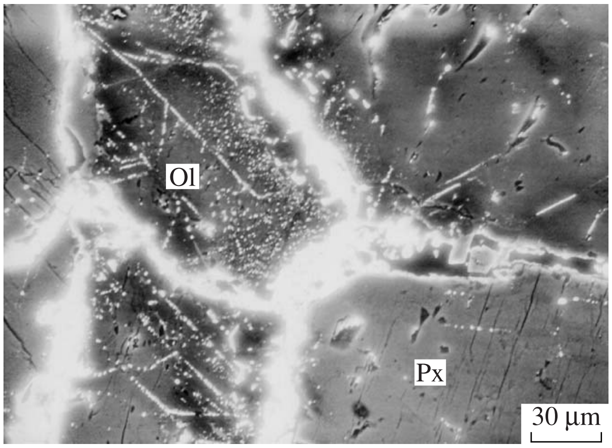

Fig. 2. A combination of interstitial and veinlet-type diamond-bearing graphite–kamacite injection in the Yamato-74659 ureilite found in Antarctica. One can see a weak influence of this injection on pyroxene (pigeonite) and intense alteration of olivine grains: development of the secondary zoning with depletion in the Fe mole fraction down to zero and release of native Ni-free iron.

from ureilites and chondrites are similar in contents of Xe, Kr, and Ar (Fig. 1). This similarity provides evidence for their genetic closeness. During the layering of planets, the embryos of fluid diamond from chondritic melts concentrated in the cores. When kamacite melts intruded the ureilite shells, the embryos served as seeds for the further growth of diamond grains, which are much larger in ureilites than in chondrites. During the emplacement of melts recorded by the injection structure of ureilites (Fig. 2), light noble gases (He, Ne) migrated more readily than heavy gases. As a result, their concentration in the ureilite-hosted diamond is much lower than in the chondrite-hosted variety. The injection of diamond-bearing kamacite melts into the pigeonite–olivine aggregate of ureilites was accompanied by a hydrogen flow that induced recrystallization of olivine with formation of inverse zoning and reduction of the Fe mole fraction to almost zero level (Table 1) with release of native iron:

$$Mg_{1.7}Fe_{0.3}SiO_4 + 0.3H_2$$
$$= 0.7Mg_2SiO_4 + 0.3MgSiO_3 + 0.3Fe + 0.3H_2O.$$

The released Fe is practically Ni-free and differs in this respect from kamacite (with 3–5 wt % Ni) intruding simultaneously with diamond. The alteration of pigeonite is more local and expressed as narrow zones irregularly penetrating the grains along fractures. This process is also accompanied by the development of native iron. The pressure created by fluid injections was high enough to provide the further growth of diamond grains characterized by abundant hydrogen inclusions in ureilites. The relationships and compositions of primary and recrystallized olivine and pyroxene grains, as well as compositions of the phases formed during the partial melting of olivine and pigeonite, are shown in Table 1 and Figs. 3 and 4. In the areas of the maximum alteration of the ureilite substrate (Table 2) at the immediate contact with graphite–kamacite veinlets, the Haverö and Novo-Urei ureilites contain tiny pyrope grains [8]. Some ureilites demonstrate intense granulation similar to hornfelsization unrelated to diamond formation. The superimposed granulation is developed in ureilites with retention of their structural pattern related to injection of the interstitial diamond-bearing graphite–kamacite melt. For example, the Haverö ureilite is almost completely transformed into the fine-

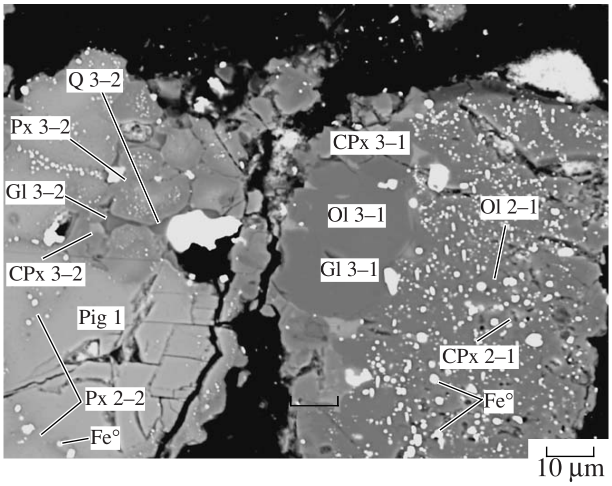

Fig. 3. The Dyalpur ureilite. Areas of intense recrystallization of pigeonite (on the left) and olivine–Fe^0 aggregate (in the center) by magnesian minerals with a cement of highly silicic glass. See Table 1 for phase compositions.

Table 1. Characteristic phase compositions (wt %) of pigeonite–olivine matrix of the Dyalpur ureilite and its complex injection structure[1]

Composition			Na_2O	MgO	Al_2O_3	SiO_2	K_2O	CaO	TiO_2	Cr_2O_3	MnO	FeO
Pigeonite–olivine matrix		Ol 1	–	44.22	–	39.93	–	0.28	–	0.60	0.58	14.39
		Pig 1	–	27.43	1.40	54.76	–	5.43	–	1.46	0.52	9.00
phase	zone											
After olivine	2-1	Ol 2-1a	–	47.89	–	40.46	–	0.38	–	0.72	0.62	9.92
		Ol 2-1b	–	53.76	–	41.93	–	0.36	–	0.76	0.59	2.60
		CPx 2-1	–	28.83	0.51	56.34	–	9.55	–	1.05	0.44	3.29
	3-1	Ol 3-1	–	54.78	–	42.04	–	0.33	–	0.53	0.50	1.82
		Px 3-1	–	34.85	0.00	58.42	–	3.64	–	0.62	0.51	1.95
		CPx 3-1	–	23.20	2.10	55.25	–	16.63	0.30	0.68	0.42	1.42
		Gl 3-1 av.(5)	1.53	14.19	19.74	55.59	0.27	7.72	–	–	0.13	0.65
After pigeonite	2-2	Px 2-2	–	29.22	1.48	55.33	–	5.29	0.27	1.35	0.46	6.61
	3-2	Px 3-2	–	34.37	0.30	57.75	–	3.24	–	0.70	0.72	2.91
		CPx 3-2	–	23.08	1.25	55.72	–	17.87	0.34	0.29	0.46	0.99
		Gl 3-2 av.(6)	0.76	10.10	10.12	71.25	0.06	4.67	–	0.04	–	2.23
		Q 3-2	–	1.89	0.86	96.59	–	0.36	–	–	–	0.30

[1] Photomicrographs and analyses in this work were performed in the Laboratory of Local Analytical Methods of the Faculty of Geology, Moscow State University, using a Jeol JSM-6480LV SEM/EDS INCA-Energy-350 (accelerating voltage 15 kV, current 15nA, and beam diameter 2 μm).

Note: (Ol) olivine, (Px) pyroxene, (Gl) glass, (Q) quartz; (2-1, 2-2) replacement zones; (3-1, 3-2) melting zones. (–) Below detection limit.

grained aggregate in some places. However, relics of the structure acquired by this ureilite during diamond formation are distinctly retained.

(3) In the course of explosive breakdown of chondritic planets into asteroids and meteorites under the impact of fluids concentrated in the melted cores at the protoplanet stage, the chondrite material was subjected to brecciation and fluid melting with the formation of various high-density phases (ringwoodite, wadsleyite, majorite, and others) in addition to garnet, which are described, for example, in glassy veinlets in the Dhofar L-chondrite [3]. This work presents the description of a fragment of olivine transformed into an assemblage of forsterite (in the center) and ringwoodite (at the margins). This process schematically corresponds to the following reaction:

$$2Mg_{1.5}Fe_{0.5}SiO_4 = Mg_{1.2}Fe_{0.8}SiO_4 \text{ (ringwoodite)} + Mg_{1.8}Fe_{0.2}SiO_4 \text{ (forsterite)}.$$

Such a transformation of olivine accompanied by complete recrystallization and redistribution of components is possible only under the effect of fluid. This interpretation contradicts the traditional concept of the development of these minerals owing to the collision of asteroids. The forsterite–ringwoodite assemblage mentioned above corresponds to a pressure of about 13 GPa. Thus, the existence of this assemblage emphasizes the strained state of chondritic and kamacite–ureilite planets due to the high concentration of fluids in their kamacite cores and the grandiosity of their explosive breakdown into asteroids and meteorites.

Table 2. Composition of minerals (wt %) from recrystallized garnet-bearing zones in ureilites

Component	Ol	Opx	CPx	Grt-1	Grt-2	Gl
SiO_2	42.97	57.89	52.62	47.25	45.58	63.43
TiO_2	–	–	0.36	0.36	–	–
Al_2O_3	–	–	5.37	20.28	23.73	1.56
Cr_2O_3	0.20	0.39	0.70	–	1.17	1.29
FeO	1.67	1.70	1.06	5.94	3.65	8.28
MnO	0.31	0.29	0.38	0.23	0.27	0.43
MgO	54.67	39.30	20.46	21.34	25.62	15.19
CaO	0.18	0.42	19.05	3.79	0.78	1.66

Note: (Grt-1) Garnet (pyrope) from the Novo-Urei meteorite; (Grt-2) garnet (pyrope) from the Haverö meteorite.

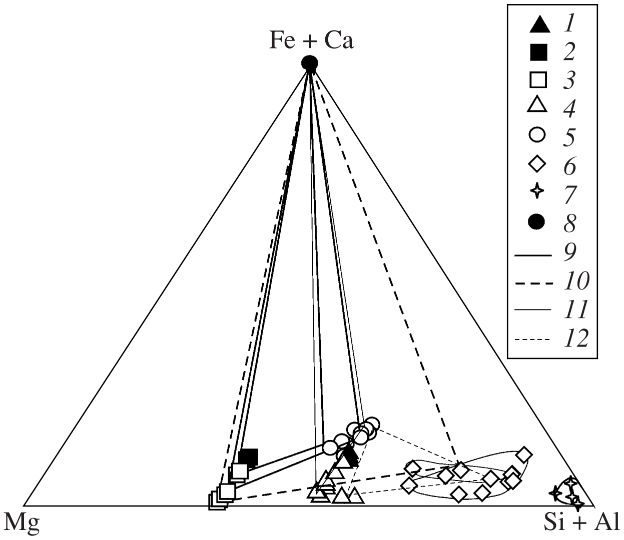

Fig. 4. The composition–paragenesis diagram of products of replacement and melting of (*1*) pigeonite and (*2*) olivine from the Dyalpur ureilite. Tie lines (*9–12*) connect mineral parageneses formed during the replacement of (*9*) olivine, (*11*) pyroxene, and phases in zones of partial melting in (*10*) olivine and (*12*) pyroxene; (*3–7*) phases from alteration zones: (*3*) olivine, (*4*) orthopyroxene, (*5*) clinopyroxene, (*6*) glass, and (*7*) silicic phase; (*8*) native Ni-free iron.

ACKNOWLEDGMENTS

The authors thank the Meteorite Committee of the Russian Academy of Sciences for the meteorite material kindly placed at our disposal for investigation.

This work was supported by the Foundation of the President of the Russian Federation for the Support of Leading Scientific Schools (project no. NSh-2849.2006.5).

REFERENCES

1. A. A. Marakushev, L. B. Granovsky, N. G. Zinovieva, et al., *Cosmic Petrology* (Nauka, Moscow, 2003) [in Russian].
2. A. A. Marakushev, N. G. Zinovieva, and L. B. Granovsky, Dokl. Earth Sci. **407A**, 434 (2006) [Dokl. Akad. Nauk **407**, 521 (2006)].
3. D. D. Badjukov, F. Brandstatter, G. Kurat, et al., in *Proceedings of the 36th Annual Lunar and Planetary Science Conference* (Lunar Planet. Inst., Houston, 2005), Vol. 36, p. 1684.
4. R. Gobel, U. Ott, and F. Begemann, J. Geophys. Res. **83**, 855 (1978).
5. G. R. Huss and R. S. Lewis, Meteoritics **29**, 791 (1994).
6. R. S. Lewis, S. Amari, and E. Anders, Geochim. Cosmochim. Acta **58**, 471 (1994).
7. O. Manuel and A. Katragada, in *Proceedings of Asteroids, Comets, Meteors—ACM 2002* (ESA Publ., Noordwijk, 2002), pp. 787–790.
8. O.B. Mitreikina, N. G. Zinovieva, and L. B. Granovsky. Antarct. Meteorite Res. **8**, 215 (1995).
9. N. Wada and J. Matsuda, Geochim. Cosmochim. Acta **62**, 2335 (1998).